CHEMISTRY
A EUROPEAN JOURNAL

DOI: 10.1002/chem.200500455

Detailed Structural Examinations of Covalently Immobilized Gold Nanoparticles onto Hydrogen-Terminated Silicon Surfaces

Yoshinori Yamanoi,[a] Naoto Shirahata,[b] Tetsu Yonezawa,*[a] Nao Terasaki,[c] Noritaka Yamamoto,[c] Yoshitaka Matsui,[d] Kazuyuki Nishio,[d] Hideki Masuda,[d] Yuichi Ikuhara,[e] and Hiroshi Nishihara*[a]

Abstract: The modification of flat semiconductor surfaces with nanoscale materials has been the subject of considerable interest. This paper provides detailed structural examinations of gold nanoparticles covalently immobilized onto hydrogen-terminated silicon surfaces by a convenient thermal hydrosilylation to form Si–C bonds. Gold nanoparticles stabilized by ω-alkene-1-thiols with different alkyl chain lengths (C_3, C_6, and C_{11}), with average diameters of 2–3 nm and a narrow size distribution were used. The thermal hydrosilylation reactions of these nanoparticles with hydrogen-terminated Si(111) surfaces were carried out in toluene at various conditions under N_2. The obtained modified surfaces were observed by high-resolution scanning electron microscopy (HR-SEM). The obtained images indicate considerable changes in morphology with reaction time, reaction temperature, as well as the length of the stabilizing ω-alkene-1-thiol molecules. These surfaces are stable and can be stored under ambient conditions for several weeks without measurable decomposition. It was also found that the aggregation of immobilized particles on a silicon surface occurred at high temperature (> 100 °C). Precise XPS measurements of modified surfaces were carried out by using a Au–S ligand-exchange technique. The spectrum clearly showed the existence of Si–C bonds. Cross-sectional HR-TEM images also directly indicate that the particles were covalently attached to the silicon surface through Si–C bonds.

Keywords: gold · nanotechnology · scanning probe microscopy · silicon · transmission electron microscopy

[a] Dr. Y. Yamanoi, Prof. Dr. T. Yonezawa, Prof. Dr. H. Nishihara
Department of Chemistry, School of Science
The University of Tokyo, 7-3-1 Hongo, Bunkyo-ku
Tokyo 113-0033 (Japan)
Fax: (+81) 3-5841-2356
E-mail: yonezawa@chem.s.u-tokyo.ac.jp
nisihara@chem.s.u-tokyo.ac.jp

[b] Dr. N. Shirahata
International Center for Young Scientists (ICYS)
National Institute for Materials Science (NMIS)
1-1 Namiki, Tsukuba, Ibaraki 305-0044 (Japan)

[c] Dr. N. Terasaki, Dr. N. Yamamoto
National Institute of Advanced Industrial Science and Technology (AIST)
1-8-31 Midorigaoka, Ikeda, Osaka 563-8577 (Japan)

[d] Dr. Y. Matsui, Dr. K. Nishio, Prof. Dr. H. Masuda
Department of Applied Chemistry, School of Engineering
Tokyo Metropolitan University
1-1 Minami-Osawa, Hachioji, Tokyo 192-0397 (Japan)

[e] Prof. Dr. Y. Ikuhara
Institute of Engineering Innovation
School of Engineering, The University of Tokyo
2-11-16 Yayoi, Bunkyo-ku, Tokyo 113-8656 (Japan)

Supporting information for this article is available on the WWW under http://www.chemeurj.org/ or from the author.

Introduction

The modification of semiconductor surfaces by the covalent attachment of organic molecules has been an active topic of investigation in the field of surface sciences.[1] The most important widespread semiconductor material is silicon. Organic monolayers immobilized on silicon substrates are crucial for microelectronics and sensors, as well as for fundamental studies. In the past, these monolayers were usually prepared by the reaction of organosilicon derivatives (such as alkylchlorosilanes, alkylalkoxysilanes, and alkylaminosilanes) with hydroxylated silicon surfaces.[2] However, this modified surface has a problem in that a silica layer, connected to the silanol groups via Si–O–Si bonds, forms on the surface. Besides the problems associated with the amorphous substrate and moisture sensitivity of the precursor molecules, the silicon dioxide thin film essentially blocks the electrical communication between the organic molecules and the silicon surface. Another useful approach to the covalent attachment of organic molecules is the hydrosilylation reaction of 1-alkenes with a hydrogen-terminated silicon (H–Si) surface.[3] Both crystalline flat H–Si(111) and

H–Si(100) surfaces,[4] as well as hydrogen-terminated porous silicon,[5] have been used as substrates. In this case, organic monolayers formed through a covalent Si–C bond provide electronic coupling between organic functionalities and the semiconductors without the interference of interfacial oxide thin film.[3–7]

Recently, much attention has centered on colloidal metal nanoparticles because of their potential applications in areas of electronics, photonics, and catalysis.[8] In particular, thiol-stabilized gold nanoparticles have become an important model system in nanomaterial research due to their stability, easy preparation and chemical versatility. Despite increasing efforts in the past few years, it is still a great challenge to fabricate well-controllable nanostructures by using colloidal particles as the structural elements. A key to achieving this goal will be the ability to assemble nanoparticles onto a desired surface to enable efficient utilization of their unique nanostructural properties. Much work has been performed to design and produce position-controlled assemblies of nanoparticles on solid surfaces, which are essential for nanodevice studies.[9,10] Ideally, it would be desirable to immobilize gold nanoparticles directly onto the surface by strong covalent bonds. Considering the potential applications of hydrogen-terminated silicon(111) surfaces mentioned above, nanoparticles could be immobilized onto a silicon surface through the highly stable Si–C bond (347 kJ mol^{-1}),[11] if we could prepare gold nanoparticles that are protected by ω-alkene-1-thiols and perform a hydrosilylation reaction. However, there have only been a few reported investigations of nanometer-sized materials attached to a silicon surface through strong Si–C bonds, one of which is our short communication.[12,13] This full paper focuses on the detailed structural examinations of immobilized gold nanoparticles on hydrogen-terminated silicon surfaces (Scheme 1) by using HR-SEM at various reaction conditions, XPS measurements and cross-sectional TEM observations.

Results and Discussion

Preparation and characterization of ω-alkene-1-thiol-covered gold nanoparticles: The use of ω-alkene-1-thiols (CH_2=$CH(CH_2)_nSH$), which undergoes reactions typical for both aliphatic thiols and olefins, is an excellent example of a strategy for immobilization onto hydrogen-terminated silicon surfaces. The aliphatic thiol parts can act as stabilizers of gold nanoparticles.[8] The C=C bonds can also participate in the hydrosilylation reaction on a hydrogen-terminated silicon surface.[3–6] In this section, we report the preparation and characterization of gold nanoparticles covered with ω-alkene-1-thiols.

We computed the energy-minimized preferred conformation of the stabilizing thiol forms and the lengths of the molecules using MM2 of Chem3D Pro V5.0. The total lengths of **1a**, **b**, and **c** (from the thiol proton to the terminal vinyl proton) were calculated to be 0.56, 0.93, and 1.6 nm, respectively (see Figure 1).

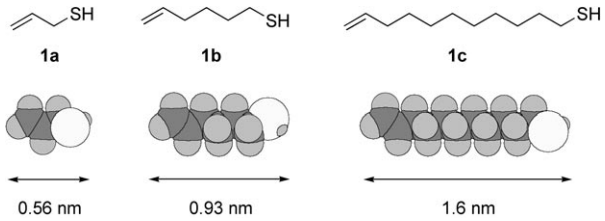

Figure 1. Energy-minimized conformation of **1a**, **1b**, and **1c**.

Gold nanoparticles **2a** were prepared by using a thiol substitution reaction between the free thiol **1a** and 1-propanethiol-stabilized gold nanoparticles (Scheme 2). The nanoparticles were prepared by a method based on the two-phase solution synthesis reported by Brust et al., and were isolated and characterized prior to the substitution reaction.[14–16] On the other hand, gold nanoparticles, **2b** and **2c**, capped with thiol **1b** or **1c**, respectively,[17] were directly synthesized by the modified Brust's two-phase method.[15,16] These gold

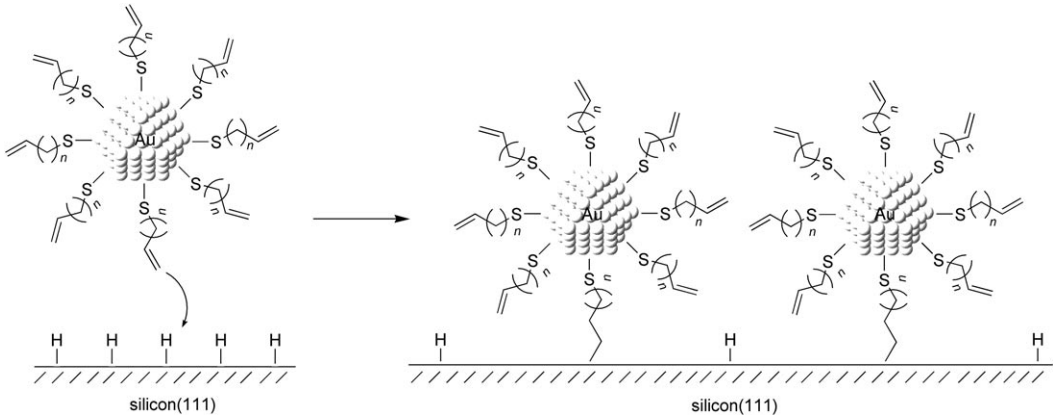

Scheme 1. Immobilization of ω-alkene-1-thiol-functionalized gold nanoparticles onto a hydrogen-terminated silicon(111) surface.

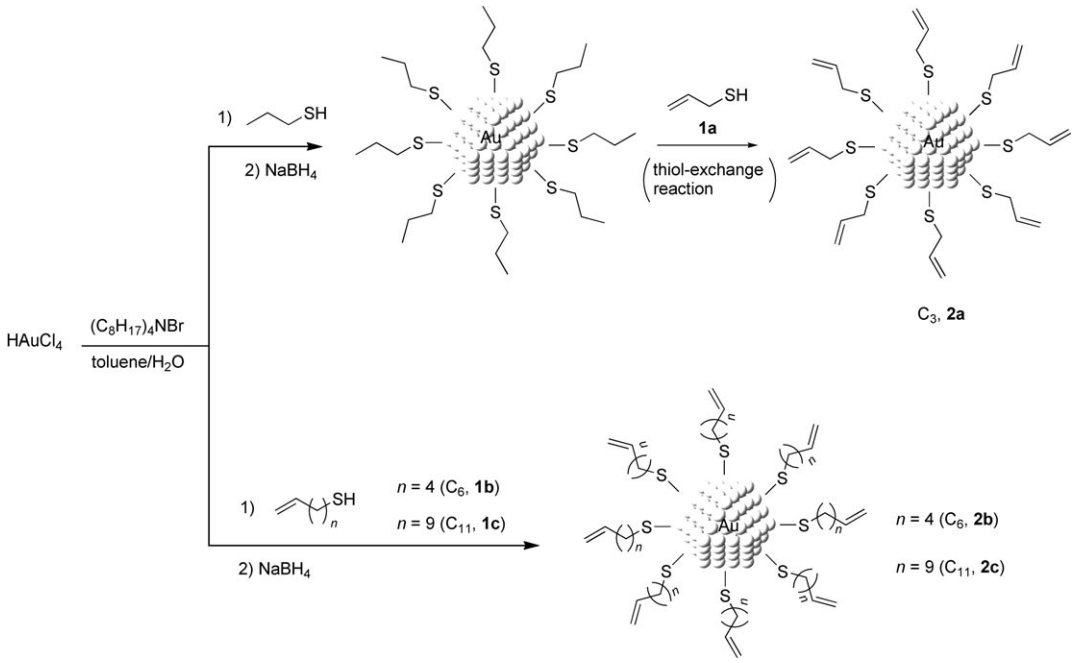

Scheme 2. Synthetic route for the preparation of gold nanoparticles stabilized by ω-alkene-1-thiols.

nanoparticles were isolated as a black powder and spectroscopically characterized. The UV-visible absorption spectra of particle dispersions in toluene were measured. All spectra exhibited peak absorbance wavelengths at around 520 nm, which is a typical plasmon resonance band for gold nanoparticles (diameter >2 nm), suggesting the formation of gold nanoparticles (Figure 2).[18]

Direct evidence concerning the size and morphology of the nanoparticles were obtained by transmission electron microscopy (TEM). Figure 3 shows the TEM images and size histograms of gold nanoparticles **2a**–**c**. These particles are spherical and two-dimensionally dispersed. The average diameters of **2a**–**c** were 3.1 ± 0.7, 2.3 ± 0.7, and 2.1 ± 0.4 nm, respectively.

^{1}H NMR spectra of these nanoparticles were measured to assess the purity of the nanoparticles, especially in order to reveal the saturation ratio of the terminal C=C unsaturated bonds of the stabilizing ω-alkene-1-thiols. Spectra obtained in $C_6D_5CD_3$ (**2a**) or $CDCl_3$ (**2b** and **2c**) showed broad peaks, and free ω-alkene-1-thiol (e.g., 2.50 ppm) was almost completely absent, as shown in Figure 4. The broadening effect is derived from the structural features of the monolayer on the gold surface. It is well known that NMR line broadening for proteins and polymers is dominated by their slow rotation in solution. Anal-

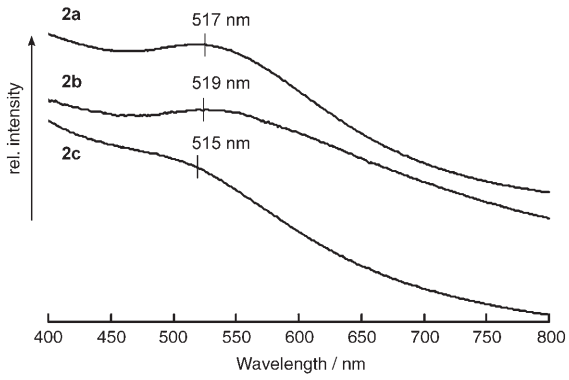

Figure 2. UV-visible absorption spectra of a toluene dispersion with **2a**, **2b**, and **2c**.

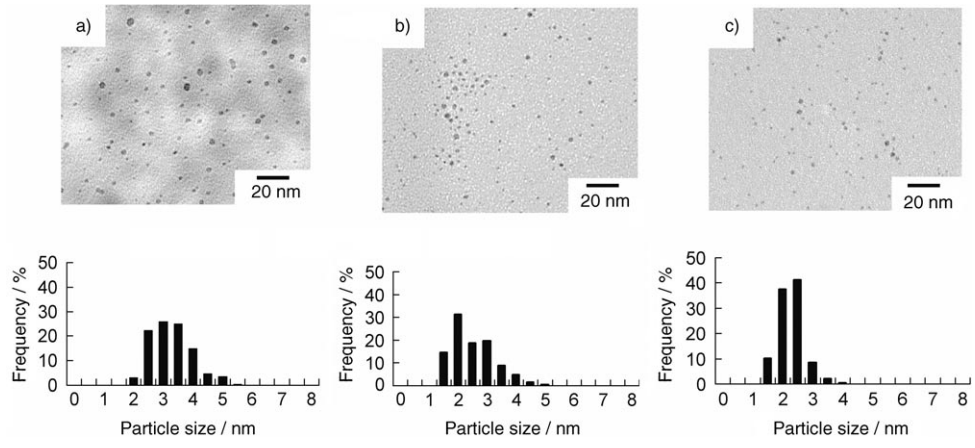

Figure 3. TEM images and size histograms of gold nanoparticles a) **2a**, b) **2b**, and c) **2c**.

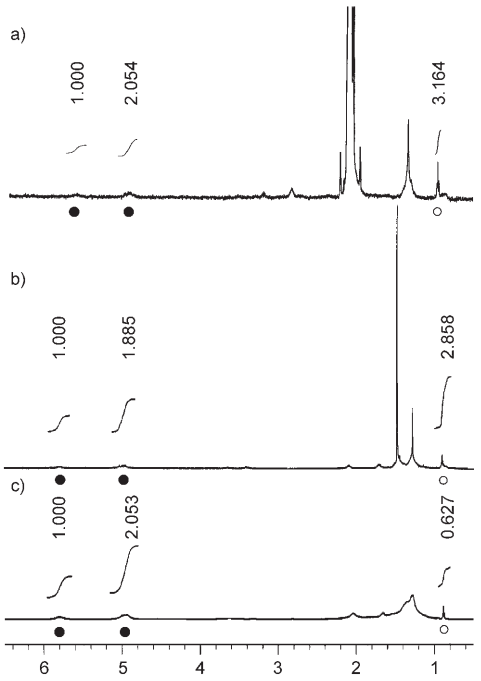

Figure 4. ^{1}H NMR spectra of gold nanoparticles a) **2a** (500 MHz, $C_6D_5CD_3$), b) **2b**, and c) **2c** (500 MHz, $CDCl_3$). ●: vinyl protons, ○: terminal methyl protons.

ogously, the aliphatic thiol-protected gold nanoparticles are slowly rotating macromolecules. These observations suggest that the hydrocarbon species derived from ω-alkene-1-thiols are densely attached to the particle surface through the sulfur atoms. Furthermore, several alkenethiols on each particle were hydrogenated during the formation of functionalized gold nanoparticles. This ratio was determined by comparing the integrated areas for the vinyl protons of alkenyl thiolates and the terminal methyl groups of alkyl thiolates. The surface ratios of alkenyl thiolates/alkyl thiolates on particles **2a**, **2b**, and **2c** were 49/51, 50/50, and 83/17 (mol/mol), respectively.

Immobilization of ω-alkene-1-thiol-stabilized gold nanoparticles—Influence of the alkyl chain length on the immobilized structure: The hydrogen-terminated silicon surface reacts with alkenes under photochemical, thermal, or catalytic conditions to generate an alkyl monolayer on the surface. The formation of such an organic monolayer was shown to be chemically robust. We have used the thermal route to coat the hydrogen-terminated silicon surface with ω-alkene-1-thiol-stabilized gold nanoparticles. The surface functionalization was carried out using the following procedures. An atomically flat hydrogen-terminated Si(111) surface was prepared by etching cleaned shards of silicon first in 1% HF solution and then in 40% ammonium fluoride as described in the literature.[11] This treatment removes the SiO_2 surface layer and etches the wafer to form an atomically flat surface. The ω-alkene-1-thiol-stabilized gold nanoparticles were first dissolved in degassed toluene (30 mg/10 mL)[19] and then added to the hydrogen-terminated silicon(111) surface at 50 °C for 24 h under a dry nitrogen atmosphere. The substrate was then rinsed with toluene, sonicated in toluene for 10 min, and dried with a stream of nitrogen. In order to avoid the oxidation of the modified surfaces, they were stored in a sealed nitrogen-filled container until analyses were performed.

Figure 5 shows HR-SEM images of gold nanoparticles immobilized onto a hydrogen-terminated silicon surface obtained by thermal hydrosilylation at various conditions. From Figure 5a, it can be seen that the immobilized colloids have an average diameter of about 10–40 nm by using C_3-alkenethiol-stabilized gold nanoparticles (**2a**). This behavior has previously been found for gold nanoparticles with short-chain surfactants (ca. 0.5 nm).[20] Traditional Ostwald ripening is a possible explanation for the changes in the size and shape of the gold nanoparticles induced by immobilization onto the silicon surface.[21] Thus, gold nanoparticles initially land on the silicon substrate in a randomly scattered way and become firmly bound to the hydrogen-terminated silicon surface through Si–C bonds. The randomly bound nanoparticles then act as seed or template particles to attract the subsequently landing particles next to them. Thus, the subsequently landing gold nanoparticles first adhere to the already-anchored particles through metallic core fusion between them. The large particles with irregular sizes and shapes were formed by the increased collision and aggregation of nucleation sites. According to the literature, this aggregation takes place as a result of a reduction of the particle surface energy when short surface-stabilizing reagents are used.[20] In contrast, no aggregation was observed in the immobilization of **2b** (Figure 5b), which indicates that nanoparticles were distributed on the silicon surface, forming nearly a monolayer coverage with approximately 15000 particles per μm^2. We found an ordered monolayer region on this modified silicon surface. The average interparticle distance was about 2.0 nm, close to twice the distance between **1b** particles (0.83 nm). It was furthermore observed that the coverage density on Si(111) decreased as the chain length of stabilizers increased from C_6 (**2b**) to C_{11} (**2c**) (Figure 5c). The low surface coverage using **2c** should be ascribed to the decrease in terminal C=C bond reactivity due to the strong hydrophobic interaction among the stabilizer molecules. According to these results, the medium chain length thiol (C_6)-stabilized gold nanoparticle (**2b**) is the most suitable for nanostructuring by a thermal hydrosilylation reaction. Subsequent TEM observations of particle dispersions after the hydrosilylation reaction showed little improvement in size distribution (Figure 6).

We also confirmed the stability of the modified silicon surfaces. Characterization of the surface after long-term (2–4 weeks) exposure to ambient laboratory conditions showed no changes.

Immobilization of 5-hexene-1-thiol-stabilized gold nanoparticles (2b)—Influence of reaction time and temperature: One of the aims of the present detailed study is to create a

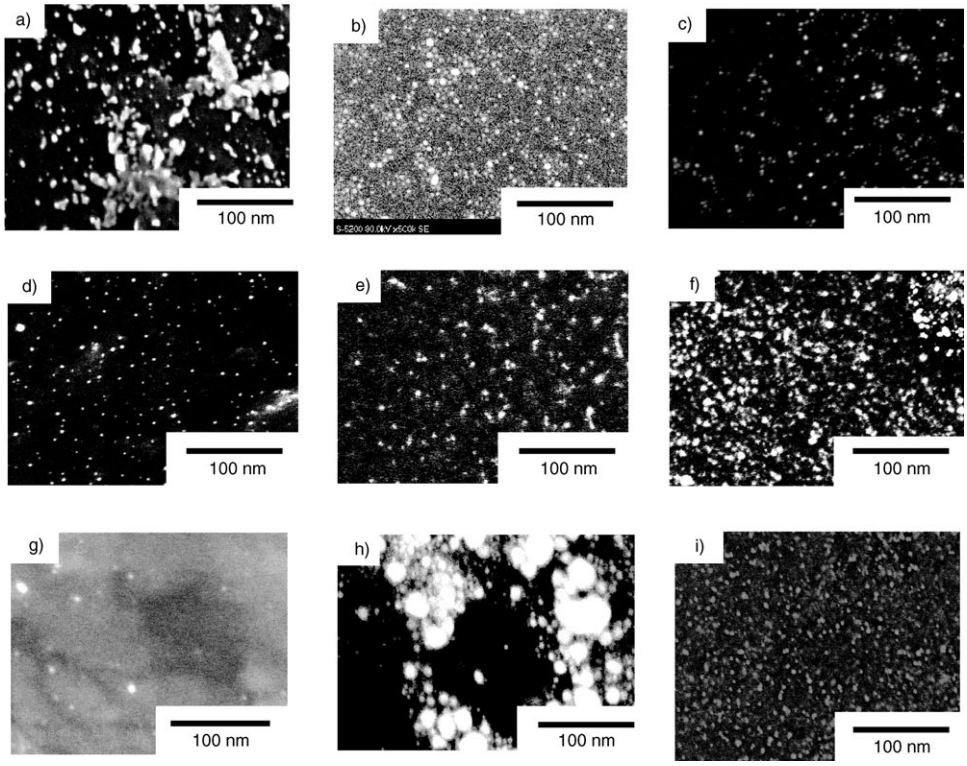

Figure 5. High-resolution SEM images after various immobilization conditions in approximately 30 mg/10 mL solutions of gold nanoparticles **2a**–**2c**. a) **2a**, 24 h, 50 °C, b) **2b**, 24 h, 50 °C, c) **2c**, 24 h, 50 °C, d) **2b**, 2 h, 50 °C, e) **2b**, 6 h, 50 °C, f) **2b**, 48 h, 50 °C, g) **2b**, 24 h, 25 °C, h) **2b**, 24 h, 100 °C, and i) **2b**, 24 h, 50 °C in the dark.

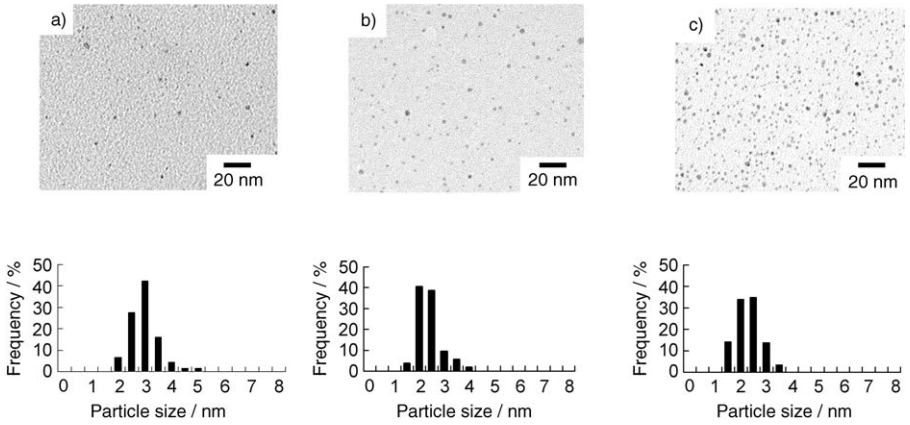

Figure 6. TEM images and size distributions of gold nanoparticles a) **2a**, b) **2b**, and c) **2c** after heating at 50 °C for 24 h in toluene.

one-particle layer without aggregation. A systematic study of the surface immobilization reaction on Si(111) is described below. To investigate the immobilization process of gold nanoparticles onto a silicon surface, we carried out the immobilization reaction at 50 °C for different periods of time. Gold nanoparticles of the type **2b**, as described in the previous section, was used as a model substrate. Figure 5d, e, b and f shows the HR-SEM images of the reacted sample after heating for 2, 6, 24, and 48 h, respectively. Obviously, the particle immobilization depended largely on reaction time. Gold nanoparticles attached in a random manner to the silicon substrate with low surface coverage at the initial stage (Figure 5d). Longer reaction time at 50 °C resulted in a significant increase in the density of the coverage. We fabricated isolated nanoparticle arrays on silicon surfaces after approximately 24 h of reaction time. After 48 h, the surface was densely covered with colloidal gold particles with self-fusion in a small partial area (Figure 5f).

The effect of reaction temperature on the fixation of gold nanoparticles (**2b**) onto a silicon surface was also explored (Figure 5g, b, and h). The hydrogen-terminated silicon surface was immersed into a toluene dispersion of **2b** (30 mg/10 mL) and heated for 24 h at temperatures ranging from 25 to 100 °C. Under these experimental conditions, particle immobilization onto the surface began at around 50 °C (Figure 5b). Below the activation temperature (25 °C), the 5-hexene-1-thiol-protected gold nanoparticles remained almost unreacted (Figure 5g). At high temperature (100 °C), the particles were aggregated and irregularly shaped, as expected. It is argued that the capping ligand is ripped off the surface of the nanoparticle during heat treatment (>100 °C) and that small spherical particles coalesce to form bigger particles.[22] The TEM observation of these refluxed gold nanoparticles in dispersion showed a small improvement in the size distribution (3.4 ± 0.8 nm, Figure 7). However, the immobilized particles were bigger than approximately 10 nm. Ostwald ripening on the silicon surface may also explain this mechanism, as described in the previous section. Recently, the photochemical attachment of 1-alkenes or 1-alkynes onto hydrogen-terminated silicon surfaces using a visible light source was reported.[23] However, the HR-SEM image of the **2b**-immobilized silicon surface was almost the same in the dark for 24 h at 50 °C as it was

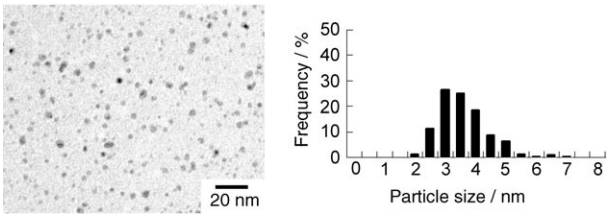

Figure 7. TEM image and size distribution of **2b** nanoparticles after heating at 100 °C for 24 h in toluene.

in visible light for 24 h at 50 °C. In this case, the immobilization process took place exclusively under thermal initiation.

Judging from these observations, silicon surfaces with well-spaced nanoparticles were apparent only up to the reaction time of 24 h at 50 °C and 30 mg/10 mL toluene solution: longer reaction time (>24 h) and higher temperature (>50 °C) led to the merging of the gold nanoparticles.

Investigation of the immobilizing structure: To establish that the particles were indeed covalently attached and not just adsorbed to the surface, the modified surfaces were subjected to ultrasonication in toluene for 1 h.[24] Since this rigorous treatment is capable of inducing bond cleavage, some erosion of particles from the surface was expected. However, HR-SEM analysis of the surface showed little change. The reaction of 1-undecanethiol (C_{11} alkanethiol)-coated gold nanoparticles with a hydrogen-terminated silicon surface at 50 °C for 24 h provided no immobilized particles, which was confirmed by HR-SEM observation.[25] This result indicates that the C=C bond in ω-alkene-1-thiol on the particle is indispensable to immobilize nanoparticles onto hydrogen-terminated silicon through the Si–C bond.

To observe the formation of Si–C bonds directly, X-ray photoelectron spectroscopy (XPS) was selected. XPS is a very useful tool for the study of covalently attached monolayers on silicon.[26] In the initial work, XPS of a particle-immobilized silicon surface was employed; however, it was found that the XPS signal from Si–C was too poor to be resolved from the C(1s) region. A ligand-exchange reaction of the **2c**-immobilized surface with a large excess amount of 1-hexadecanethiol ($C_{16}H_{33}SH$) was then applied to remove all gold nanoparticles without cleavage the Si–C bonds on the silicon surface. The HR-SEM measurement of the silicon surface indicated successful removal of gold nanoparticles (Figure 8a and b). The XPS results for this system are also shown in Figure 8c and d. The freshly prepared hydrogen-terminated Si(111) surface shows no Si–C bond and only a

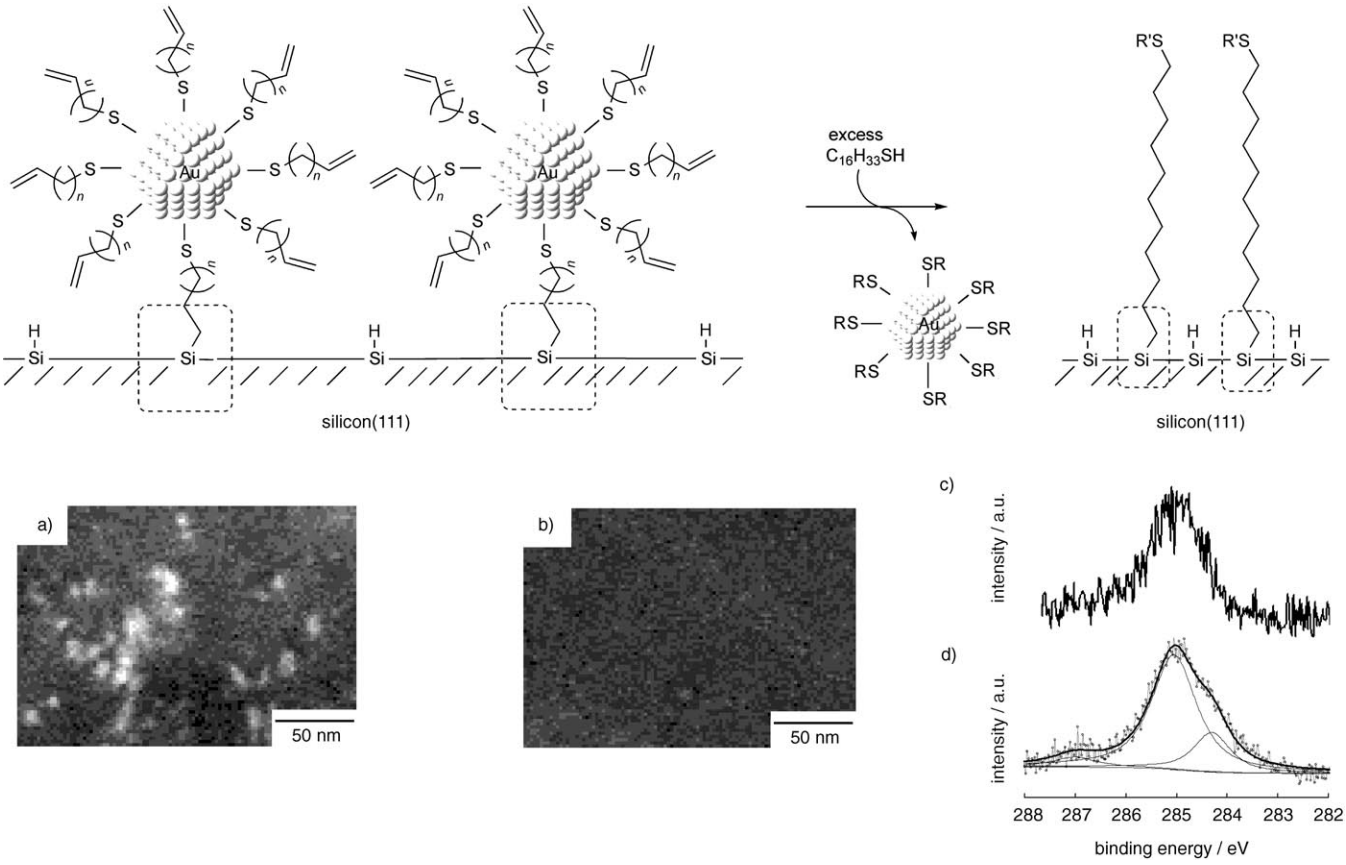

Figure 8. a) SEM images comparing **2c** immobilized silicon surface ($n=9$), b) the silicon surface after removal of **2c** with 1-hexadecanethiol, c) a carbon (1s) narrow XPS scan for the hydrogen-terminated silicon surface and d) the modified silicon surface after the cleavage of gold nanoparticle **2c** using a large excess amount of 1-hexadecanethiol.

small C–C signal, which is presumably due to physically adsorbed hydrocarbons (Figure 8c). As shown in Figure 8d, the C(1s) core-level spectrum of the surface can be fitted with two peaks having binding energies at approximately 284 and 285 eV, attributable to the C–Si and C–C species, respectively. This spectrum shows the carbon 1s signal from the silicon(111) surface, modified by the attachment of 11-undecene-1-thiol. From this result, the ω-alkene-1-thiol-stabilized gold nanoparticles were thought to be attached to the hydrogen-terminated silicon surface through Si–C bonds.[27] As a control, the Si(111)-H surface was exposed to neat 1-hexadecanethiol (10 mL) and 10-undecene-1-thiol in toluene (0.3 mg/10 mL) at room temperature for 7 d. No Si–C bond signal was detected by XPS measurement in either case.[28]

Apart from conventional XPS, gold nanoparticles immobilized onto silicon surfaces were also directly observed with cross-sectional TEM.[29] Figure 9 shows cross-sectional TEM images of **2b** immobilized onto a silicon surface. The overview image in Figure 9a demonstrates that a uniform gold nanoparticle submonolayer is formed on the Si(111) surface. The high-resolution cross-sectional TEM image is shown in Figure 9b. This image clearly shows **2b** gold nanoparticles in the near surface layer, surrounded by 5-hexene-1-thiol (**1b**). Thus, the distance between the particles and the surface in Figure 9b was estimated to be 0.95 nm, in fairly good agreement with the expected distance (0.90 nm).[30]

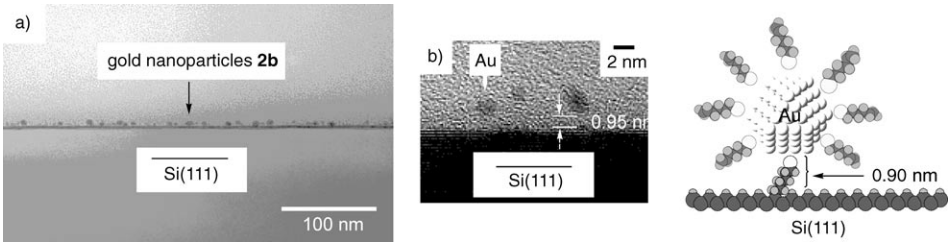

Figure 9. a) Cross-sectional TEM image of **2b** gold nanoparticles immobilized onto a silicon surface. b) Calculated and experimentally determined height in the formation of **2b** nanoparticles immobilized onto a silicon surface.

These observations provide strong evidence that these particles are directly immobilized onto a hydrogen-terminated silicon surface through Si–C bonds.

Conclusion

Herein we presented detailed structural observations of covalently immobilized gold nanoparticles on hydrogen-terminated silicon surfaces by a thermal hydrosilylation reaction under an inert atmosphere. A series of ω-alkene-1-thiol-protected gold nanoparticles was successfully prepared using a method based on the two-phase solution synthesis and spectroscopically characterized. The modified silicon surface was easily obtained by thermal hydrosilylation of the hydrogen-terminated silicon(111) surface with these particles in toluene. The effect of the length of the stabilizer thiols, reaction temperature, and reaction time are important factors influencing the modified silicon surfaces. Using HR-SEM, XPS with removal of particles by an Au–S ligand-exchange method, and cross-sectional TEM analysis, we confirmed that the gold nanoparticles were directly attached to the silicon surface through robust Si–C bonds. Our total structural examinations of the immobilization of nanomaterials onto silicon surfaces should become a standard combination of analytical methods. This surface-modification method is generic in the sense that it should be easy to extend to a broad range of nanosized compounds that expose unsaturated carbon–carbon bonds. Gold nanoparticles are expected to behave as quantum dots, and we believe that our approach for successful and reproducible fabrication of nanostructures will bring the manufacture of nanoparticle-based devices a step closer to realization.

Experimental Section

Materials and chemicals: All experiments were carried out in a dry nitrogen atmosphere. All starting materials were purchased from Aldrich or other reagent manufacturers and used without further purification. All organic solvents were distilled from CaH_2 and stored over MS 4 Å. Deionized water (resistivity higher than 18.2 MΩcm) was purified with a Millipore Milli-Q water system. N-type silicon wafers with (111) orientation were obtained from Chiyoda Koeki Co. Ltd. and used as a substrate after suitable chemical etching.

General methods: *NMR spectroscopy*: ^{1}H NMR studies of nanoparticles and their precursors were recorded on a Bruker DRX-500 spectrometer at room temperature. Chemical shifts in ppm were referenced to tetramethylsilane (0.00 ppm) as an internal standard. *FT-IR spectroscopy*: FT-IR spectra were recorded on a Jasco FT/IR-620v spectrometer. *Mass spectrometry*: MS (EI) measurements were recorded on a Shimadzu GCMS-QP5000A. *Elemental analysis*: Elemental analysis of the products was performed on a Yanaco MT-6 CHN recorder at the Elemental Analysis Center of the University of Tokyo. *UV-visible spectroscopy*: UV-visible spectra were recorded using a Hewlett-Packard 8453 UV/Vis spectrometer at 20 °C in the visible region to find the location and intensity of the surface plasmon resonance peak for the particles.

Structural examinations: *TEM*: The TEM images were recorded at 200 kV by using a Hitachi HF-2000. The TEM samples of gold nanoparticles were prepared at room temperature by depositing a droplet of a toluene solution of particles onto a carbon film supported on a copper grid. The micrographs were then analyzed by using Scion image analysis software. More than 500 particles were used in the statistical analyses to determine the size distribution, which indicated the mean diameter and its standard deviation. *HR-SEM*: The SEM images were recorded at 30 kV by using a Hitachi S-5000 or S-5200. The preparation of specimens is described below. *Cross-sectional HR-TEM*: The cross-sectional TEM images were taken at 300 kV using a Topcon. The samples for cross-sectional TEM images were prepared by a conventional method. *XPS*: Sample surfaces were characterized by using X-ray photoelectron spectroscopy (XPS; ULVAC-PHI, Quantum-2000 system) with monochromatic $Al_{K\alpha}$ ($h\nu = 1486.6$ eV) radiation. The monochromatic Al anode was operated at 15 kV and 20 W. Static point acquisitions were collected with a

100 μm² analysis area. Spectra were recorded at constant pass energy of 5.85 eV, with a step size of 0.025 eV. The core-level signals were obtained at a photoelectron takeoff angle of 45° (with respect to the sample surface). During operation of the spectrometer, the pressure in the analysis chamber was less than 4×10^{-10} Torr. All the binding energies were normalized to that of the Si 2p peak appearing at 99.3 eV, which was referenced to a p-type Si wafer. The resultant XPS profiles were analyzed by using a Gaussian–Lorentzian fit program.

Synthesis

ω-Alkene-1-thiol 1b and 1c: 5-Hexene-1-thiol (**1b**) and 10-undecene-1-thiol (**1c**) were each prepared from corresponding alkenyl bromide substrate according to the well-known thiourea route.[31] A typical synthesis was carried out as follows. Thiourea (7.61 g, 100 mmol) and alkenyl bromide (20 mmol) were added to ethanol (300 mL) in a two-neck flask equipped with a reflux condenser. The reaction mixture was heated to reflux for 24 h. The reaction was allowed to cool to room temperature, and then 2 M NaOH aqueous solution (50 mL) was added. The solution was heated to reflux for 24 h. The reaction was monitored by silica gel thin-layer chromatography (TLC). After cooling to room temperature, the solution was treated with 1 M HCl to pH 7. The organic layer was separated, and the aqueous layer was extracted with CH_2Cl_2 three times. The combined extracts were dried over Na_2SO_4. The solvent was evaporated under slightly reduced pressure, and the residue was dissolved in hexane. The solution was passed through a short column packed with silica gel (hexane) to give the corresponding ω-alkene-1-thiol in moderate to good yield.

Compound 1b: colorless oil (0.79 g, 34%); ^{1}H NMR ($CDCl_3$, 500 MHz): $\delta=5.80$ (ddt, $J=17.2$, 10.3, 6.7 Hz, 1H), 5.02 (ddt, $J=17.1$, 2.0, 1.6 Hz, 1H), 4.97 (ddt, $J=10.2$, 2.0, 1.1 Hz, 1H), 2.54 (q, $J=7.4$ Hz, 2H), 2.07 (q, $J=7.2$ Hz, 2H), 1.63 (quin, $J=7.4$ Hz, 2H), 1.49 (quin, $J=7.5$ Hz, 2H), 1.34 (t, $J=7.9$ Hz, 1H); IR (neat): $\tilde{\nu}$ = 3076, 2928, 2855, 1641, 991, 911 cm^{-1}; EI-MS: m/z: 115 $[M-H]^+$.

Compound 1c: colorless oil (3.09 g, 83%); ^{1}H NMR ($CDCl_3$, 500 MHz): δ = 5.81 (ddt, $J=17.1$, 10.3, 6.7 Hz, 1H), 4.99 (dd, $J=17.1$, 1.7 Hz, 1H), 4.93 (d, $J=10.0$ Hz, 1H), 2.52 (q, $J=7.4$ Hz, 2H), 2.04 (q, $J=7.1$ Hz, 2H), 1.61 (quin, $J=7.3$ Hz, 2H), 1.39–0.92 (m, 13H); IR (neat): $\tilde{\nu}$ = 3076, 2920, 2850, 1462, 910, 723 cm^{-1}; EI-MS: m/z: 185 $[M-H]^+$.

Gold nanoparticles 2a: Gold nanoparticles **2a** were prepared by the ligand-exchange reaction of allyl mercaptan with 1-propanethiol-protected gold nanoparticle.[13] The 1-propanethiol-stabilized gold nanoparticles were synthesized by using a modified version of a method in the literature.[15] Hydrogen tetrachloroaurate(III) tetrahydrate (6.00 g, 14.6 mmol) in deionized water (200 mL) was added to a vigorously stirred solution of tetra-*n*-octylammonium bromide (22.4 g, 41.0 mmol) in toluene (600 mL). The yellow aqueous solution immediately became clear and the toluene phase turned brown. The organic phase was transferred into a 1 L round-bottom flask, and 1-propanethiol (1.5 mL, 16.8 mmol) was added to the solution. Sodium borohydride (3.18 g, 84.0 mmol) in deionized water (200 mL) was slowly added to a vigorously stirred solution. The resulting solution was stirred for 3 h at room temperature. The solvent was removed under reduced pressure without exceeding a temperature of 50 °C. The dark residue was suspended in ethanol (1 L) and kept in a refrigerator at −10 °C overnight. The precipitate was collected by filtration on a membrane filter and washed thoroughly with ethanol. The purified gold nanoparticles were isolated as a black powder (3.48 g). Further surface functionalization was achieved by a ligand-exchange reaction with 1-propanethiol-protected gold nanoparticle and allyl mercaptan. 1-Propanethiol-protected gold nanoparticles (529 mg) were dissolved in CH_2Cl_2 (10 mL). To this solution was added allyl mercaptan (0.5 mL), and the reaction mixture was stirred at room temperature for 2 h. The solvent was evaporated under reduced pressure. The dark residue was suspended in ethanol (1 L) and kept overnight in a refrigerator at −10 °C. The precipitate was collected by filtration on a membrane filter and washed thoroughly with ethanol. Gold nanoparticles **2a** were obtained as a black powder (504 mg). The nanoparticles were characterized by ^{1}H NMR, FT-IR, UV-vis, elemental analysis, and TEM.

Compound 2a:[16] ^{1}H NMR gave very broad peaks. The ratio of alkyl thiolates to alkenyl thiolates on the particles was 51:49. ^{1}H NMR ($C_6D_5CD_3$, 500 MHz, selected peaks): δ = 5.70–5.61 (brs, 1H), 5.04–4.88 (brs, 2H); IR (KBr): $\tilde{\nu}$ = 3074, 2952, 2908, 1631, 1412, 912 cm^{-1}; UV/Vis (toluene): λ_{max} = 517 nm; elemental analysis calcd (%) for $C_{342}H_{570}Au_{459}S_{114}$ ($Au_{459}(C_3H_5S)_{114}$): C 4.16, H 0.58; found C 5.10, H 0.85.

Gold nanoparticles 2b and 2c: Gold nanoparticles **2b** and **2c** were also synthesized as described by Brust et al.[15] Hydrogen tetrachloroaurate(III) tetrahydrate (1.00 g, 2.4 mmol) in deionized water (75 mL) was added to a vigorously stirred solution of tetra-*n*-octylammonium bromide (6.02 g, 11 mmol) in toluene (250 mL). The yellow aqueous solution became clear immediately and the toluene phase turned brown. The organic phase was transferred into a 1 L round-bottom flask, and ω-alkene-1-thiol (2.4 mmol) was added to the solution. Sodium borohydride (0.25 g, 6.6 mmol) in deionized water (50 mL) was slowly added to a vigorously stirred solution. The resulting solution was stirred for 3 h at room temperature. The organic phase was separated and dried over sodium sulfate, and the solvent was removed under reduced pressure without exceeding a temperature of 50 °C. The dark residue was suspended in ethanol (1 L) and kept in a refrigerator at −10 °C overnight. The precipitate was collected by filtration on a membrane filter and washed thoroughly with ethanol. This process was repeated to ensure the removal of any free ω-alkene-1-thiol in the product. The complete removal of unabsorbed ω-alkene-1-thiol from the nanoparticles was ascertained by ^{1}H NMR. The purified gold nanoparticles were kept in powder form and redispersed into organic solvents (e.g., toluene, $CHCl_3$, CH_2Cl_2, and THF). Finally, the nanoparticles were characterized by ^{1}H NMR, FT-IR, UV/Vis, elemental analysis, and TEM.

Compound 2b: 445 mg, 78%; ^{1}H NMR gave very broad peaks. The ratio of alkyl thiolates to alkenyl thiolates on particles was 50:50. ^{1}H NMR ($CDCl_3$, 500 MHz, selected peaks): δ = 5.90–5.69 (brs, 1H), 5.03–4.95 (brs, 2H), 3.34–3.31 (m, 2H), 1.71–1.66 (m, 2H), 1.39–1.37 (m, 2H), 0.84–0.81 (m, 2H); IR (KBr): $\tilde{\nu}$ = 3074, 2918, 2848, 1637, 1414, 906 cm^{-1}; UV/Vis (toluene): λ_{max} = 519 nm; elemental analysis calcd (%) for $C_{552}H_{1012}Au_{309}S_{92}$ ($Au_{309}(C_6H_{11}S)_{92}$): C 9.28, H 1.39; found C 8.91, H 1.53.

Compound 2c:[17] 520 mg, 80%; ^{1}H NMR gave very broad peaks. The ratio of alkyl thiolates to alkenyl thiolates on particles was 17:83. ^{1}H NMR ($CDCl_3$, 500 MHz, selected peaks): δ = 5.80 (brs, 1H), 4.94 (brs, 2H), 2.03–0.87 (m, 2H); IR (KBr): $\tilde{\nu}$ = 3074, 2920, 2848, 1412, 908 cm^{-1}; UV/Vis (toluene): λ_{max} = 515 nm; elemental analysis calcd (%) for $C_{583}H_{1113}Au_{140}S_{53}$ ($Au_{140}(C_{11}H_{21}S)_{53}$): C 18.72, H 3.00; found C 18.83, H 3.08.

Preparation of silicon substrate: A typical experimental procedure for the immobilization of gold nanoparticles onto a hydrogen-terminated silicon surface is as follows. The hydrogen-terminated silicon(111) surface was prepared by chemical etching as previously reported.[11] Silicon(111) wafers were cut into squares (10 mm × 10 mm). The silicon substrates were cleaned ultrasonically in toluene for 10 min. The substrates were etched in 1% HF aqueous solution at 70 °C for 1 min (in a Teflon vessel) and further etched in 30% NH_4F aqueous solution at room temperature for 5 min (in a Teflon vessel) to remove surface oxide and to etch the surface anisotropically. The fresh hydrogen-terminated silicon surface was transferred under nitrogen into a Schlenk tube containing gold nanoparticles in toluene (30 mg/10 mL) and kept at 50 °C for 24 h. After cooling to room temperature, the sample was removed from the solution, rinsed with toluene, and sonicated in toluene for 10 min. Finally, the modified silicon substrate was rinsed briefly with toluene and dried in a stream of argon gas. ***CAUTION**! HF is very dangerous, particularly in contact with skin, and should be handled with extreme care.*

Detachment of gold nanoparticles from 2c-immobilized silicon surfaces by a Au–S ligand-exchange method: The freshly prepared hydrogen-terminated silicon(111) surface was immersed into the toluene dispersion of gold nanoparticle **2c** (30 mg/10 mL) and heated to 100 °C for 4 d. After immobilization, the silicon wafer was removed from the solution, rinsed thoroughly with toluene, cleaned sonically in toluene for 10 min, and dried under a flow of nitrogen. The cleavage of the gold nanoparticles from this specimen was accomplished in a nitrogen atmosphere by the addition of 1-hexadecanethiol (10 mL). The reaction was carried out at room temperature for 7 d. Subsequently, the silicon piece was removed from the solution, rinsed thoroughly with toluene, sonicated in toluene

for 10 min, and dried under a flow of nitrogen. The specimen was then promptly subjected to HR-SEM and XPS measurement.

Acknowledgements

The authors thank Hitachi Science Systems and Hitachi High Technologies for their experimental assistance with the HR-SEM observation. This work was financially supported in part by a Grant-in-Aid for Scientific Research from the Ministry of Education, Culture, Sports, Science, and Technology, Japan. T.Y. also thanks the Mitsubishi Chemical Corporation Fund for financial support.

[1] For recent reviews, see: a) D. Y. Petrovykh, F. J. Himpsel, "Self-assembled Nanostructures at Silicon Surface" in *Encyclopedia of Nanoscience and Nanotechnology, Vol. 9* (Ed.: H. S. Nalwa), American Scientific Publishers, Stevenson Ranch, California, **2004**, pp. 497–528; b) C. H. Choi, M. S. Gordon, "Chemistry on Silicon Surface" in *Chemistry of Organic Silicon Compounds, Vol. 3* (Eds.: Z. Rappoport, Y. Apeloig), Wiley, **2001**, pp. 821–851.

[2] For recent reviews, see: a) P. K. Jal, S. Patel, B. K. Mishra, *Talanta* **2004**, *62*, 1005–1028; b) F. Schreiber, *Prog. Surf. Sci.* **2000**, *65*, 151–256; c) A. Ulman, *Chem. Rev.* **1996**, *96*, 1533–1554.

[3] For recent reviews, see: a) J. M. Buriak, *Chem. Rev.* **2002**, *102*, 1271–1308; b) D. D. M. Wayner, R. A. Wolkow, *J. Chem. Soc. Perkin Trans. 2* **2002**, 23–34; c) N. Shirahata, A. Hozumi, T. Yonezawa, *Chem. Rec.* **2005**, *5*, 145–159.

[4] For representative examples, see: a) M. R. Linford, C. E. D. Chidsey, *J. Am. Chem. Soc.* **1993**, *115*, 12631–12632; b) M. R. Linford, P. Fenter, P. M. Eisenberger, C. E. D. Chidsey, *J. Am. Chem. Soc.* **1995**, *117*, 3145–3155; c) C. H. de Villeneuve, J. Pinson, M. C. Bernard, P. Allongue, *J. Phys. Chem. B* **1997**, *101*, 2415–2420; d) A. B. Sieval, A. L. Demirel, J. W. M. Nissink, M. R. Linford, J. H. van der Mass, W. H. de Jeu, H. Zuilhof, E. J. R. Sudhölter, *Langmuir* **1998**, *14*, 1759–1768; e) R. Boukherroub, S. Morin, F. Bensebaa, D. D. M. Wayner, *Langmuir* **1999**, *15*, 3831–3835; f) A. B. Sieval, R. Linke, H. Zuilhof, E. J. R. Sudhölter, *Adv. Mater.* **2000**, *12*, 1457–1460.

[5] For representative examples, see: a) J. M. Buriak, *Adv. Mater.* **1999**, *11*, 265–267; b) H. C. Choi, J. M. Buriak, *Chem. Mater.* **2000**, *12*, 2151–2156; c) J. M. Buriak, M. P. Stewart, T. W. Geders, M. J. Allen, H. C. Choi, J. Smith, D. Raftery, L. T. Canham, *J. Am. Chem. Soc.* **1999**, *121*, 11491–11502; d) J. M. Schmeltzer, L. A. Porter, M. P. Stewart, J. M. Buriak, *Langmuir* **2002**, *18*, 2971–2974; e) R. Boukherroub, A. Petit, A. Loupy, J.-N. Chazalviel, F. Ozanam, *J. Phys. Chem. B* **2003**, *107*, 13459–13462; f) J. E. Bateman, R. D. Eagling, D. R. Worrall, B. R. Horrocks, A. Houlton, *Angew. Chem.* **1998**, *110*, 2829–2831; *Angew. Chem. Int. Ed.* **1998**, *37*, 2683–2685; g) M. P. Stewart, J. M. Buriak, *Angew. Chem.* **1998**, *110*, 3447–3450; *Angew. Chem. Int. Ed.* **1998**, *37*, 3257–3260.

[6] For representative recent examples of stable Si–C linked monolayers with hydrogen-terminated silicon surfaces, see: a) T. Yamada, T. Inoue, K. Yamada, N. Takano, T. Osaka, H. Harada, K. Nishiyama, I. Taniguchi, *J. Am. Chem. Soc.* **2003**, *125*, 8039–8042; b) B. Fabre, D. D. M. Wayner, *Langmuir* **2003**, *19*, 7145–7146; c) P. T. Hurley, A. E. Ribbe, J. M. Buriak, *J. Am. Chem. Soc.* **2003**, *125*, 11334–11339; d) W. H. Yu, E. T. Kang, K. G. Neoh, *Langmuir* **2004**, *20*, 8294–8300; e) B. J. Eves, Q.-Y. Sun, G. P. Lopinski, H. Zuilhof, *J. Am. Chem. Soc.* **2004**, *126*, 14318–14319; f) D. Xu, E. T. Kang, K. G. Neoh, A. A. O. Tay, *Langmuir* **2004**, *20*, 3324–3332; g) C. M. Yam, J. Cho, C. Cai, *Langmuir* **2004**, *20*, 1228–1233.

[7] For Si–C bond formation by using cycloaddition of organic molecules with semiconductor surfaces, see: a) F. Tao, G. Q. Xu, *Acc. Chem. Res.* **2004**, *37*, 882–893; b) S. F. Bent, *J. Phys. Chem. B* **2002**, *106*, 2830–2842; c) R. J. Hamers, S. K. Coulter, M. D. Ellison, J. S. Hovis, D. F. Padowitz, M. P. Schwartz, C. M. Greenlief, J. N. Russell, Jr., *Acc. Chem. Res.* **2000**, *33*, 617–624.

[8] For recent reviews, see: a) *Nanoparticles* (Ed.: G. Schmid), Wiley, Weinheim, **2004**; b) J. C. Love, L. A. Estroff, J. K. Kriebel, R. G. Nuzzo, G. M. Whitesides, *Chem. Rev.* **2005**, *105*, 1103–1169; c) B. L. Cushing, V. L. Kolesnichenko, C. J. O'Connor, *Chem. Rev.* **2004**, *104*, 3893–3946; d) M. C. Daniel, D. Astruc, *Chem. Rev.* **2004**, *104*, 293–346; e) G. Schmid, B. Corain, *Eur. J. Inorg. Chem.* **2003**, 3081–3098; f) N. A. Kotov, "Layer-by-layer Assembly of Nanoparticles and Colloids: Intermolecular Interactions, Structure, and Material Perspectives" in *Multilayer Thin Films* (Eds.: G. Decher, J. B. Schlenoff), Wiley, Weinheim, **2003**, pp. 207–269; g) T. Yonezawa, N. Toshima, "Polymer-stabilized Metal Nanoparticles" in *Advanced Functional Molecules and Polymers* (Ed.: H. S. Nalwa), Gordon and Breach, London (UK), **2001**, pp. 65–86; h) A. C. Templeton, W. P. Wuelfing, R. W. Murray, *Acc. Chem. Res.* **2000**, *33*, 27–36.

[9] For example, see: a) E. W. L. Chan, D.-C. Lee, M.-K. Ng, G. Wu, K. Y. C. Lee, L. Yu, *J. Am. Chem. Soc.* **2002**, *124*, 12238–12243; b) E. W. L. Chan, L. Yu, *Langmuir* **2002**, *18*, 311–313; c) H. X. He, H. Zhang, Q. G. Li, T. Zhu, S. F. Y. Li, Z. F. Liu, *Langmuir* **2000**, *16*, 3846–3851; d) A. C. Templeton, F. P. Zamborini, W. P. Wuelfing, R. W. Murray, *Langmuir* **2000**, *16*, 6682–6688; e) J. A. Harnisch, A. D. Pris, M. D. Porter, *J. Am. Chem. Soc.* **2001**, *123*, 5829–5830; f) T. A. Taton, R. C. Mucic, C. A. Mirkin, R. L. Letsinger, *J. Am. Chem. Soc.* **2000**, *122*, 6305–6306; g) T. Okamoto, I. Yamaguchi, *J. Phys. Chem. B* **2003**, *107*, 10321–10324; h) S. Chen, R. Pei, T. Zhao, D. J. Dyer, *J. Phys. Chem. B* **2002**, *106*, 1903–1908; i) H. Tanaka, M. Mitsuishi, T. Miyashita, *Langmuir* **2003**, *19*, 3103–3105; j) Q. Li, J. Zheng, Z. Liu, *Langmuir* **2003**, *19*, 166–171; k) R. D. Tilley, S. Saito, *Langmuir* **2003**, *19*, 5115–5120; l) S. Chen, R. W. Murray, *J. Phys. Chem. B* **1999**, *103*, 9996–10000; m) Y. Joseph, I. Besnard, M. Rosenberger, B. Guse, H.-G. Nothofer, J. M. Wessels, U. Wild, A. Knop-Gericke, D. Su, R. Schlögl, A. Yasuda, T. Vossmeyer, *J. Phys. Chem. B* **2003**, *107*, 7406–7413; n) J. Zheng, Z. Chen, Z. Liu, *Langmuir* **2000**, *16*, 9673–9676.

[10] Electrophoretic deposition, see: a) M. Yamada, T. Tadera, K. Kubo, H. Nishihara, *Langmuir* **2001**, *17*, 2363–2370; b) M. Yamada, H. Nishihara, *Langmuir* **2003**, *19*, 8050–8056.

[11] R. T. Sanderson, *Chemical Bonds and Bond Energy*, Academic Press, New York, **1976**.

[12] Preliminary communication: Y. Yamanoi, T. Yonezawa, N. Shirahata, H. Nishihara, *Langmuir* **2004**, *20*, 1054–1056.

[13] a) Miller et al. reported the preparation of the covalently bonded C_{60} monolayers on silicon surface, see: W. Feng, B. Miller, *Langmuir* **1999**, *15*, 3152–3156; b) Quite recently, Altavilla et al. reported the monolayers of ω-alk-1-ene-silane functionalized magnetite (Fe_3O_4) nanoparticles covalently linked to a hydrogen-terminated silicon-(111) surface by a thermal hydrosilylation reaction. See: C. Altavilla, E. Ciliberto, D. Gatteschi, C. Sangregorio, *Adv. Mater.* **2005**, *17*, 1084–1087.

[14] For examples of ligand-exchange reactions on monolayer-protected gold nanoparticles, see: a) M. J. Hostetler, A. C. Templeton, R. W. Murray, *Langmuir* **1999**, *15*, 3782–3789; b) R. S. Ingram, M. J. Hostetler, R. W. Murray, *J. Am. Chem. Soc.* **1997**, *119*, 9175–9178; c) M. J. Hostetler, S. J. Green, J. J. Stokes, R. W. Murray, *J. Am. Chem. Soc.* **1996**, *118*, 4212–4213.

[15] M. Brust, M. Walker, D. Bethell, D. J. Schiffrin, R. Whyman, *J. Chem. Soc. Chem. Commun.* **1994**, 801–802.

[16] One referee asked for an explanation about these experiments. Although gold nanoparticles **2a** were prepared according to Brust's two-phase method from $HAuCl_4$ and allyl mercaptan in our previous report, the reproducibility of the method was poor. Accordingly, we prepared **2a** by thiolate substitution reaction in CH_2Cl_2. From this result, we noticed that significant particle aggregation was observed when the fraction of allyl mercaptan was increased (more than approximately 60%). On the other hand, high reproducibility was found for the synthesis of gold nanoparticle **2b** and **2c** by the use of Brust's two-phase method. Therefore, these particles were not prepared by ligand-exchange reaction.

[17] McCarley et al. reported the preparation of 10-undecene-1-thiol-protected gold nanoparticles. J. S. Peanasky, R. L. McCarley, *Langmuir* **1998**, *14*, 113–123.
[18] a) M. M. Alvarez, J. T. Khoury, T. G. Schaaff, M. N. Shafigullin, I. Vezmar, R. L. Whetten, *J. Phys. Chem. B* **1997**, *101*, 3706–3712; b) T. G. Schaaff, M. N. Shafigullin, J. T. Khoury, I. Vezmar, R. L. Whetten, W. C. Cullen, P. N. First, C. J. Gutiérrez-Wing, Ascensio, M. J. Jose-Yacamán, *J. Phys. Chem. B* **1997**, *101*, 7885–7891.
[19] Gold nanoparticles **2a**–**2c** were added in great excess (more than 1000 times the required quantity).
[20] For recent examples, see: a) P. Buffat, J.-P. Borel, *Phys. Rev. A* **1976**, *13*, 2287–2298; b) L. J. Lewis, P. Jensen, J.-L. Barrat, *Phys. Rev. B* **1997**, *56*, 2248–2257; c) C. J. Kiely, J. Fink, M. Brust, D. J. Schiffrin, *Nature* **1998**, *396*, 444–446; d) T. Yonezawa, S. Onoue, N. Kimizuka, *Chem. Lett.* **2002**, 1172–1173.
[21] A. Stella, P. Cheyssac, R. Kofman, "Fundamental Properties and Developments of Metallic and Semiconducting Nanoparticles" in *Science and Technology of Thin Films* (Eds.: F. C. Matacotta, G. Ottaviani), World Scientific, River Edge, NJ, **1996**, pp. 517–587.
[22] a) M. M. Maye, W. Zheng, F. L. Leibowitz, N. K. Ly, C.-J. Zhong, *Langmuir* **2000**, *16*, 490–497; b) M. M. Maye, C.-J. Zhong, *J. Mater. Chem.* **2000**, *10*, 1895–1901; c) T. Teranishi, S. Hasegawa, T. Shimizu, M. Miyake, *Adv. Mater.* **2001**, *13*, 1699–1701.
[23] a) Q.-Y. Sun, L. C. P. M. de Smet, B. van Lagen, M. Giesbers, P. C. Thüne, J. van Engelenburg, F. A. de Wolf, H. Zuilhof, E. J. R. Sudhölter, *J. Am. Chem. Soc.* **2005**, *127*, 2514–2523; b) Q.-Y. Sun, L. C. P. M. de Smet, B. van Lagen, A. Wright, H. Zuilhof, E. J. R. Sudhölter, *Angew. Chem.* **2004**, *116*, 1376–1379; *Angew. Chem. Int. Ed.* **2004**, *43*, 1352–1355; c) M. P. Stewart, J. M. Buriak, *J. Am. Chem. Soc.* **2001**, *123*, 7821–7830.
[24] The use of ultrasound in the simple removal of contaminants attached as surface coatings is well known, see: T. J. Mason, J. P. Lorimer, *Sonochemistry*, Wiley, Chichester (UK), **1988**.
[25] See Supporting Information for the SEM image.
[26] a) J. Terry, M. R. Linford, C. Wigren, R. Cao, P. Pianetta, C. E. D. Chidsey, *Appl. Phys. Lett.* **1997**, *71*, 1056–1058; b) N. Shirahata, T. Yonezawa, Y. Miura, K. Kobayashi, K. Koumoto, *Langmuir* **2003**, *19*, 9107–9109; c) N. Shirahata, T. Yonezawa, W.-S. Seo, K. Koumoto, *Langmuir* **2004**, *20*, 1517–1520; d) A. Bansal, X. Li, S. I. Yi, W. H. Weinberg, N. S. Lewis, *J. Phys. Chem. B* **2001**, *105*, 10266–10277; e) N. Y. Kim, P. E. Laibinis, *J. Am. Chem. Soc.* **1998**, *120*, 4516–4517; f) R. L. Cicero, M. R. Linford, C. E. D. Chidsey, *Langmuir* **2000**, *16*, 5688–5695; g) R. Boukherroub, S. Morin, F. Bensebaa, D. D. M. Wayner, *Langmuir* **1999**, *15*, 3831–3835; h) H. B. Liu, R. J. Hamers, *Surf. Sci.* **1998**, *416*, 354–362.
[27] We also carried out a ligand-exchange reaction of the **2a** or **2b**-immobilized silicon surface with 1-hexadecanethiol, followed by XPS measurement of the modified silicon surface. The signal of Si–C could not be observed.
[28] The reactions of 1-hexadecanethiol (neat) and 1-undecenethiol in toluene (3 mg/10 mL) with a hydrogen-terminated silicon(111) surface were carried out at room temperature for 7 d. The signal of Si–C bonds was not detected by XPS measurement in both cases. See Supporting Information for the XPS.
[29] For cross-sectional TEM observations of gold nanoparticles on surfaces, see: a) K. Sun, S. Zhu, R. Fromknecht, G. Linker, L. M. Wang, *Mater. Lett.* **2004**, *58*, 547–550; b) S. H. Cho, S. Lee, D. Y. Ku, T. S. Lee, B. Cheong, W. M. Kim, K. S. Lee, *Thin Solid Films* **2004**, *447–448*, 68–73.
[30] The calculated distance between particle **2b** and the silicon surface was obtained by a semi-empirical calculation (MOPAC, PM3, closed-shell-restricted) in Chem3D Pro.
[31] A. J. Speziale, *Org. Synth.* **1963**, *Vol. V*, 401.

Received: April 22, 2005
Revised: June 25, 2005
Published online: October 6, 2005

